



# Physically crosslinked polyvinyl alcohol–dextran blend xerogels: Morphology and thermal behavior

Ezatollah Fathi<sup>a</sup>, Nahid Atyabi<sup>a</sup>, Mohamad Imani<sup>b,\*</sup>, Zeinab Alinejad<sup>b</sup>

<sup>a</sup> Department of Clinical Pathology, Faculty of Veterinary Medicine, University of Tehran, Tehran, Iran

<sup>b</sup> Novel Drug Delivery Systems Department, Iran Polymer and Petrochemical Institute, P.O. Box 14975-112, Tehran, Iran

## ARTICLE INFO

### Article history:

Received 24 August 2010

Received in revised form 26 October 2010

Accepted 9 November 2010

Available online 16 November 2010

### Keywords:

Polyvinyl alcohol

Dextran

Freeze–thaw

Xerogels

Thermal properties

## ABSTRACT

Physically crosslinked hydrogels composed of different amounts of dextran in PVA matrix were prepared by applying freeze–thaw cycles to their aqueous solutions. Morphology, thermal properties and FTIR spectra of the resulting blend xerogels were examined by SEM, DSC, TGA and FTIR spectroscopy. Blend xerogels containing 10% (w/w) dextran showed more compatibility/miscibility according to SEM and DSC results. The  $T_g$  of the xerogels did not show any significant changes with increased dextran content. Introducing dextran into the freeze–thawed PVA structure affected crystal size distribution of PVA; and hence thermal degradation behavior of the xerogels. An increase in dextran content resulted in broader crystal size distribution; better and still lower thermal stability in comparison to virgin PVA and freeze–thawed PVA, respectively.

© 2010 Elsevier Ltd. All rights reserved.

## 1. Introduction

Hydrogels are three-dimensional polymeric networks which absorb and retain high volume of water. Hydrophilic structure or domains are absolutely needed for these polymeric networks to become hydrated in aqueous environments hence creating the hydrogel structure (Hennink & van Nostrum, 2002). In swollen state, these materials become soft and rubbery, resembling a living tissue and some possess excellent biocompatibility (Soppinath & Aminabhavi, 2002). Upon their excellent biological properties, a great number of reports has appeared in scientific literature since 1960s when the first report on the application of poly(2-hydroxyethyl methacrylate) hydrogels as contact lens was published (Wichterle & Lim, 1960). Considering the term “network” implies a crosslinked structure which may be achieved by a chemical reaction (e.g., radical polymerization, chemical reaction of complementary groups, using high energy irradiation or enzymatic reactions) or physical bonds such as ionic interactions, crystallization of the polymeric chains, design of amphiphilic block and graft copolymers, hydrogen bonds between chains or protein interactions which in turn have their own advantages as well as some shortcomings (Hennink & van Nostrum, 2002).

In recent decades, there has been an increasing interest in physically crosslinked gels (Berger, Reist, Mayer, Felt, & Gurny, 2004; De Jong, van Eerdenbrugh, van Nostrum, Kettenes-van den

Bosch, & Hennink, 2001; Molina, Suming, Martinez, & Vert, 2001; Peppas & Scott, 1992; Van Tomme, van Steenberg, De Smedt, van Nostrum, & Wim, 2005). The main reason is to avoid the use of chemical crosslinking agents. These agents are not only often toxic compounds which have to be removed/extracted from the final gels before application but also can affect the integrity of the substances when entrapped (e.g., proteins, cells). To create physically crosslinked gels, different methods such as ionic interaction (Berger et al., 2004; Van Tomme et al., 2005), amphiphilic block and graft copolymers (Molina et al., 2001), stereocomplex formation (De Jong et al., 2001; Hennink, De Jong, Bos, Veldhuis, & van Nostrum, 2004), freezing–thawing (Hassan & Peppas, 2000; Peppas & Scott, 1992; Yokoyama, Masada, Shimamura, Ikawa, & Monobe, 1985), etc., have been investigated. In this regard; polyvinyl alcohol (PVA) holds tremendous promise as a hydrogel-forming polymer via crystallization owing to its non-toxic and hydrophilic nature (Peppas, 1987).

Different methods have been reported in preparation of PVA-based hydrogels including radiation crosslinking (Park & ChangNho, 2003; Yoshii, Zhanshan, Isobe, Shinozaki, & Makuuchi, 1999), chemical reaction with glyoxal (Teramoto, Saitoh, Kuroiwa, Shibata, & Yosomiya, 2001), bifunctional reagents, e.g., glutaraldehyde (Dai & Barbari, 1999; Peppas & Benner, 1980), or borates (Korsmeyer & Peppas, 1981). Aqueous solution of PVA would be eventually transformed to a low strength gel upon long storage at room temperature however; this does not meet many applications' requirements where mechanical properties are important. In a method, pioneered by Peppas et al. (Peppas, 1975), semi-crystalline gels were prepared by exposing PVA aqueous solution

\* Corresponding author. Tel.: +98-21 4458 0036; fax: +98-21 4458 0036.

E-mail address: [M.Imani@ippi.ac.ir](mailto:M.Imani@ippi.ac.ir) (M. Imani).

to repeated freezing and thawing cycles which induced crystallization and resulted in a network structure with the quasi-permanent crystallites which act as physical crosslinking sites in the network. This method is the preferred route to prepare an “ultrapure” network without the using any toxic crosslinking agents with tunable mechanical properties (Yokoyama et al., 1985). Mechanical properties of the gel increase with the temperature, number of freezing/thawing cycles, polymer solution concentration and its molecular weight hence; different mechanical properties and erosion time up to six months were obtained (Hassan & Peppas, 2000).

Many oppositely working parameters should be considered at the same time to develop a polymeric system suitable for specific applications such as drug delivery or tissue engineering, to include physico-mechanical properties, biodegradability, swelling and release behaviors which equally dictate a compromise between these demands by optimization and differently needed modifications. Blending of PVA with PVP (Park & ChangNho, 2003), chitosan (Kim, Park, & Kim, 2003a), poly(*N*-isopropylacrylamide) (Kim, Park, & Kim, 2003b), carboxymethyl chitosan (Zhao et al., 2003), and alginate is previously reported to meet such demands. Blending with alginate is reported for BSA-loaded PVA gels which are simply obtained by dissolution of proteins in the aqueous polymer solution followed by freezing–thawing cycles. Gel properties can be modulated by varying blend ratios, when, e.g., mechanical strength is increased with increased alginate concentration the amount of drug released is simultaneously decreased. BSA is reported to be released by a Fickian diffusion process with preservation of its conformation (Peppas & Scott, 1992).

The effect of dextran on the properties of PVA hydrogels, prepared by freezing–thawing method is reported for low concentration regimes of PVA (2.5%, w/w solution) and dextran, i.e., 9% (w/w) (with respect to PVA) in its maximum content (Cascone, Maltinti, & Barbani, 1999). In the light of such contribution; the results of PVA–dextran blend hydrogels are explained in details in this paper. The gels were prepared physically using freeze–thaw cycles at high concentration of PVA (20%, w/w) and high dextran (10, 20, and 30%, w/w) contents. The blend hydrogels were characterized by scanning electron microscopy (SEM), Fourier transform infrared (FTIR), differential scanning calorimetry (DSC) and thermal gravimetric analysis (TGA).

## 2. Experimental

### 2.1. Materials

PVA of 72,000 g mol<sup>−1</sup> nominal molecular weight and 98% degree of hydrolysis was obtained from Merck Chemicals (Darmstadt, Germany). Dextran 40 USP ( $M_w = 36,644$  and  $M_n = 20,190$  g mol<sup>−1</sup>) was provided by Pharmacosmos A/S (Holbaek, Denmark). De-ionized water of conductivity below 6 microsiemens was used throughout this research and prepared in house using a YOUNG LIN AquaMAX 370 (YOUNG LIN Instruments, Anyang, Korea).

### 2.2. Preparation of hydrogels

PVA–dextran gels were prepared by dissolving PVA (20 g) in 100 mL of de-ionized water. Dextran in different percentages (0, 10, 20, and 30%, w/w) was added to this solution which will be so-called Dex0, Dex10, Dex20 and Dex30 for abbreviation, hereafter. The final mixture was maintained at 120 °C and 1.5 bar pressure for 2 h in an autoclave for complete dissolution along with sterilization (Manabu & Takehisa, 2002). The resulting mixture was then cooled down at room temperature, and kept at −20 °C for 20 h. The homogeneous solution after freezing was held at room temperature

(25 °C for 4 h). Freezing and thawing cycles were repeated 4 times to provide mechanically acceptable gels for further experiments (Peppas, 1975). The gels were frozen in liquid nitrogen for 6 min, before being lyophilized (VaCo 5 laboratory freeze dryer, ZIRBUS technologies, Harz, Germany) at −50 °C for 48 h. All samples were left in de-ionized water for 72 h to extract leachable sol fraction, i.e., mostly dextran from matrix.

### 2.3. Fourier-transform infrared spectroscopy (FTIR)

FTIR spectra (4000–400 cm<sup>−1</sup>) of the neat and blend xerogels were acquired using an Equinox 55 spectrophotometer (Bruker, Germany) at 4 cm<sup>−1</sup> resolution and 32 scans at room temperature. All samples were freeze fractured using liquid nitrogen, crushed to a fine powder then mixed with KBr in 50:50 weight ratio of KBr to the crushed powder and pressed into transparent disks (≈150 mg weight) with a diameter of 13 mm by applying a force of 105 N. All measurements were made in transmittance mode.

### 2.4. Thermal analysis

Differential scanning calorimetry (DSC) was performed using a NETZSCH DSC 200 F3 (NETZSCH, Selb, Germany) under nitrogen gas flow rate of 50 mL/min and at a heating rate of 10 °C/min from −70 °C up to complete decomposition at 600 °C. The experiment was performed in three cycles to eliminate thermal history of the samples. The temperature cycles were comprised of three steps which started at first from −70 °C to 130 °C, followed by the next cycle of 130 °C to −70 °C and the final run of −70 °C to complete decomposition at 600 °C. The  $T_g$  of the samples like other fundamental thermal properties was determined from the third heating run as mid-point in heat flow baseline change (Lucke, Tebmar, Schnell, Schmeer, & Pferich, 2000). Thermal properties of the PVA–dextran xerogels were characterized by thermogravimetric analysis (TGA) using a Pyris 1 equipment (Perkin Elmer, Waltham, USA) under nitrogen atmosphere at a heating rate of 10 °C/min.

### 2.5. Scanning electron microscopy (SEM)

Phase distribution and morphology of the gels (surface and cross-section) were analyzed by scanning electron microscopy (SEM) employing a Vega II XMU instrument (Tescan, Czech Republic) using 15 kV voltage for secondary electron imaging after coating with Au–Pd in 200 and 1500 magnification ratios.

### 2.6. Statistical analysis

Statistical analysis was performed using MiniTab software (Release 11.12, Minitab Inc., State College, PA, USA). Outliers were detected and excluded from interpretations according to the *T* procedure (Sanford Bolton, 1991) using the following equation:

$$T_n = \frac{X_n - \bar{X}}{S} \quad (1)$$

where,  $X_n$  either the smallest or largest value,  $\bar{X}$  is the mean value and  $S$  is the standard deviation. Values of  $T_n$  were compared with tabulated *T* values for *p* value less than 0.05.

## 3. Results and discussion

### 3.1. Morphology

Surface morphology of the xerogels in different formulations is clearly shown in scanning electron micrographs as depicted in Fig. 1. According to these micrographs, Dex0 samples provide a

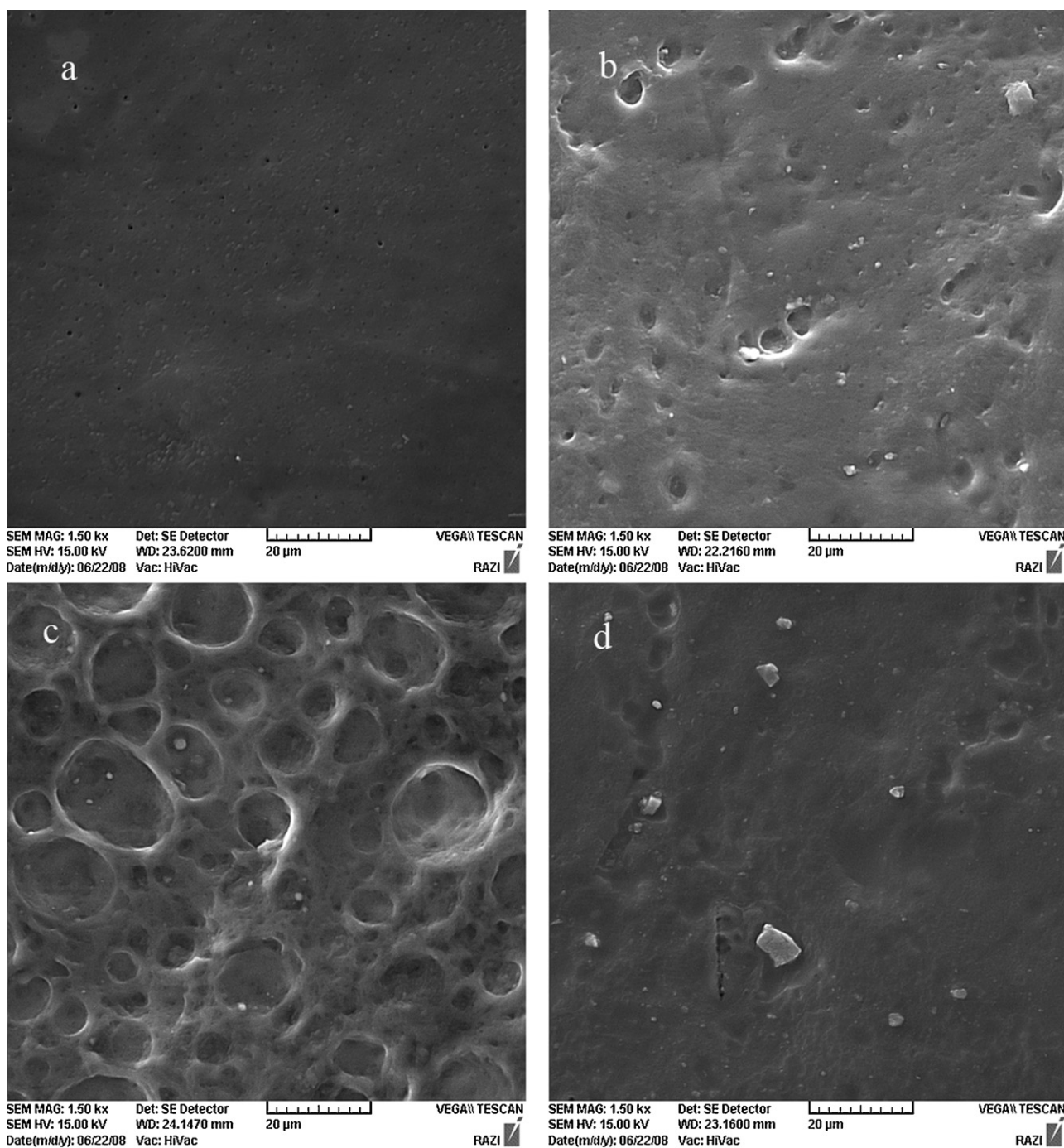


**Fig. 1.** SEM micrograph showing the surface morphology of different PVA/dextran blend hydrogels (a) Dex0, (b) Dex10, (c) Dex20 and (d) Dex30 (magnification ratio =  $\times 1500$ ).

very smooth surface with pore diameters in the range of 1–1.5  $\mu\text{m}$  after sol fraction extraction and freeze drying (Fig. 1a). Distribution of pore sizes is narrow in these samples in contrast to Dex10 and Dex20 samples (Fig. 1b and c) which can be attributed to the extraction of dextran particles in different agglomeration numbers. Number of pores and their sizes are also increased significantly to provide pores within 5–8  $\mu\text{m}$  range diameters for Dex10 and more than 20  $\mu\text{m}$  for Dex20 samples. Presence of dextran particles is evident as a separate phase in the concentration range from 10% to 30% (w/w) which indicates that dextran and PVA are not completely miscible and excess free dextran has to be separated as shown in Figs. 1d and 2d. Miscibility of dextran ( $M_w = 78,000$ ) in PVA ( $M_w = 85,000$ , DH = 87.4%) was previously examined by Cascone and

Maltinti who reported 9% (w/w) (dextran/PVA) miscibility limit (Cascone et al., 1999). In Dex30 samples a uniform and smooth surface was observed and channeling was the dominant phenomenon as evident in surface and cross-section morphologies (Figs. 1d and 2d). This morphological change can be attributed to the re-ordered crystalline phase of the PVA matrix at 30% (w/w) dextran hydrogels. The presence of pores in regular form indicates that despite dextran they significantly perturb the formation of PVA crystallites because of their partial miscibility.

Using freeze-fracture method in liquid nitrogen smooth and mirror-like fracture surfaces was produced without any fractals or cracks due to brittle nature of the produced xerogels. In contrast to Dex0 samples which showed little or no macroporosity in



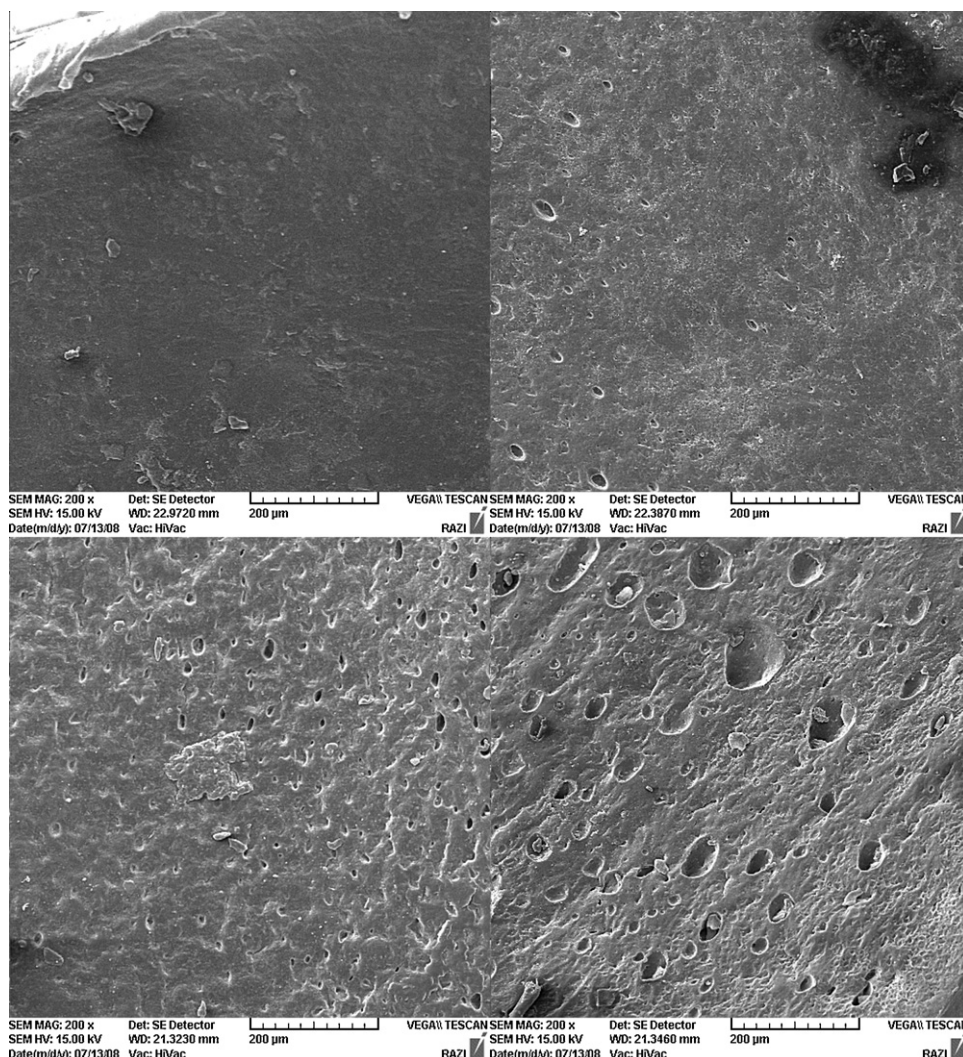


**Fig. 2.** SEM micrograph showing the cross-section morphology of different PVA/dextran blend hydrogels (a) Dex0, (b) Dex10, (c) Dex20 and (d) Dex30 (magnification ratio =  $\times 200$ ).

their cross-sections (Fig. 2a); Dex10 and Dex20 samples exhibited uniformly dispersed porous structures upon extraction of dextran (Fig. 2b and c). Pore sizes in the bulk of the xerogels increased with higher dextran loading probably upon more agglomeration of the porogen in higher loadings. Channeling was the dominant phenomenon in Dex30 samples which could be attributed to the exceeding dispersed phase ratio, *i.e.*, dextran from the limit dictated by percolation theory. The channels seem to be interconnected as illustrated in Fig. 2d. The presence of dextran as agglomerated particles is evident in all the dextran containing samples.

### 3.2. Thermal properties

#### 3.2.1. Differential scanning calorimetry

DSC thermograms showing changes in the glass transition temperature for PVA and PVA hydrogels (Dex0 samples) are depicted in Fig. 3a. Adopting a freezing–thawing procedure to fabricate the crosslinked polymeric networks has culminated to a significant reduction in  $T_g$  from 85 °C for neat PVA to 26 °C for networks which means a rubbery or nearly rubbery xerogels in ambient condition. This significant reduction in  $T_g$  can be assigned to the physical crosslinks provided upon partial crystallization of PVA chains and consequent increases in the free volume throughout amorphous regions or possibly due to reductions in hydrogen bonding in the

same amorphous domains. A small amount (10%, w/w) of dextran is sufficient to increase the  $T_g$  value from 26 °C to 40 °C in PVA xerogel blends. As tabulated in Table 1, the  $T_g$  value remained constant at 40 °C with higher dextran content of the xerogels. Increases in  $T_g$  upon inclusion of 10% (w/w) dextran can be attributed to higher  $T_g$  of dextran and its miscibility with PVA matrix. This indicates that PVA and dextran are only partially miscible in the xerogel state however; exact value for miscibility could not be determined using the designed compositions. In compositions beyond 10% (w/w) (*e.g.*, Dex20 and Dex30) only physical blends of the two polymers is present which do not affect glass transition temperature. The same

**Table 1**

Thermal properties of PVA–Dex blend xerogels according to the DSC thermograms<sup>a</sup>.

Sample	$T_g$ (°C)	$T_\beta$ (°C)	$T_{m1}$ (°C)	$T_{\text{shoulder}}$ (°C)	$T_{m2}$ (°C)
PVA	85.99	149	219	258	273
Dextran	227	–	–	–	285
DEx0	26.85	160	197 and 211	251	268
Dex10	40.19	167	197 and 214	260	274
Dex20	40.09	166	197 and 219	260	274 and 304
Dex30	42.07	167	197 and 219	260	274 and 304

<sup>a</sup>  $T_{m1}$  and  $T_{m2}$  are reported for maximum values observed for first and second melting endotherms.

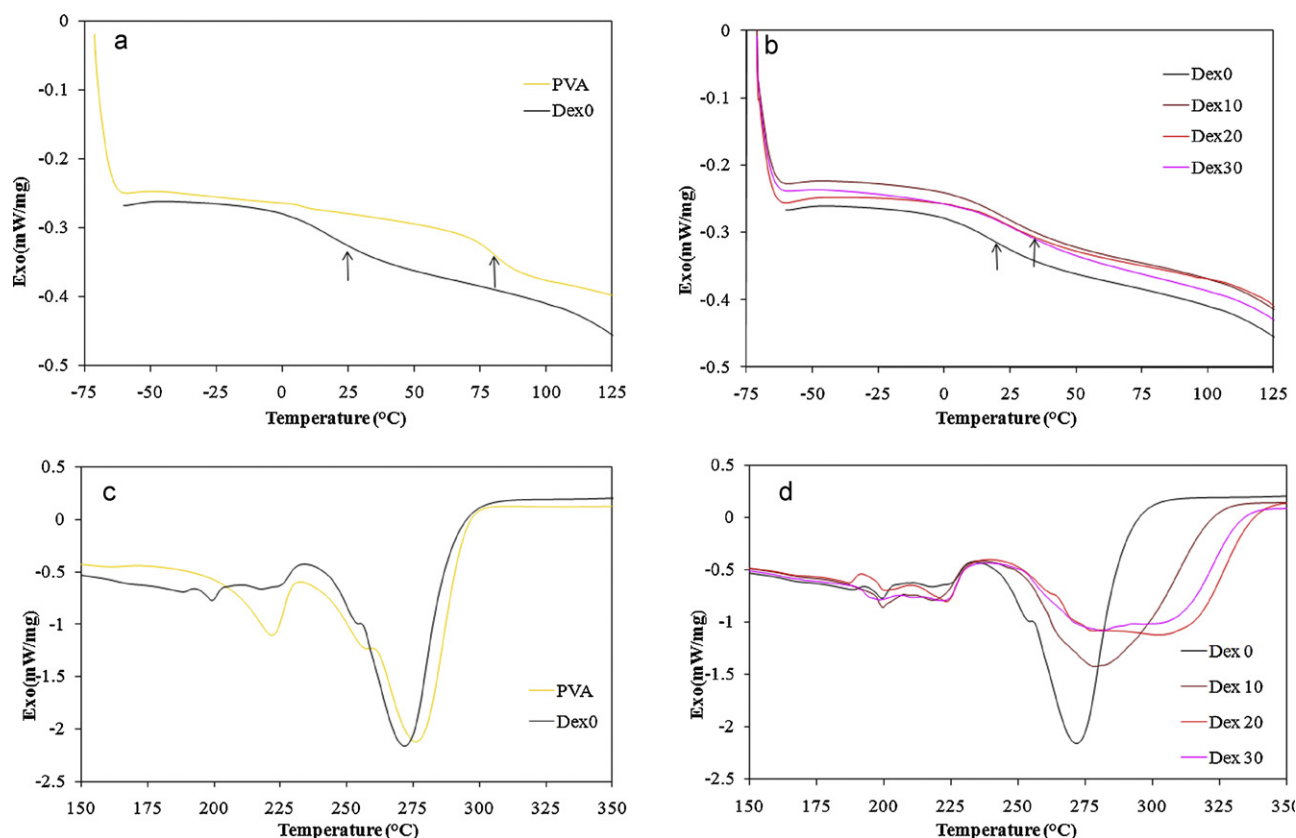


**Fig. 3.** DSC thermogram showing changes in glass transition temperature for PVA and PVA xerogel (a);  $T_g$  of samples with different content of dextran (b); changes in crystallization and melting behavior of PVA and PVA xerogels (c) and crystallization and melting behavior of samples with different content of dextran (d).

result is reported for chitosan/PVA hydrogel where at first  $T_g$  of chitosan/PVA blend hydrogel increased with chitosan content and then it remained constant (Cascone et al., 1999).

The second transition that can be observed in Fig. 3c and d is the relaxation occurring at 149°C for neat PVA and 167°C for Dex0 designated as  $\beta$  relaxation which is due to the relaxation in the PVA crystalline domains. The freezing–thawing cycles do not necessarily increase the overall degree of crystallinity and they just stabilize those existing crystals (Hassan & Peppas, 2000), so that this shift could be due to the higher degrees of crystallinity or more ordered structure of Dex0 compared to the neat PVA. Because relaxation of more ordered crystals needs more energy hence, the relaxation temperature shifts to higher temperatures. The results are shown in Table 1 which elucidate that  $\beta$  relaxation temperature does not change significantly upon increases in dextran content above 10% (w/w). The observed phenomenon can be attributed to the partial miscibility of dextran and PVA that do not apparently interact beyond the critical miscibility limit.

The third relaxation in PVA hydrogel blends is related to the melting of the crystalline regions. Determination of  $T_m$  is difficult for PVA-based materials upon their decomposition at temperatures above 130°C (Marten, 1985) but according to the popular estimation method for the equilibrium  $T_m$ , polymer samples are usually annealed at various temperatures before  $T_m$  determinations to represent  $T_m$  as a function of annealing temperature (Hassan & Peppas, 2000). However, our hydrogel preparation method was a kind of heat treatment and for neat PVA two peak endotherms were observed (Fig. 3a). Melting temperature for neat PVA was observed at 219°C (the lower temperature side peak) and 273°C (the higher temperature side peak) as shown in Fig. 3c. The first endothermic characteristic peak was partially removed upon physical crosslinking in the pure PVA xerogels due to their crosslinked structure or

partial crystallization, however; both melting temperatures shifted to lower temperatures after crosslinking by freezing–thawing method. This is more likely due to the fact that crystalline regions before freezing–thawing were less ordered and larger in thickness but upon freezing–thawing, became more ordered and therefore more packed crystals were formed. Thus, decreasing crystal size results in crystals of relatively low melting temperature. It is noteworthy that melting peaks were sharpened upon freezing–thawing as an indicator of more ordered crystal structure. A shoulder at 258°C for neat PVA and 251°C for Dex0 samples were observed at the higher temperature side peak. This is probably due to the fact that after 130°C, especially in the second peak; melting of PVA crystallites happens simultaneously with degradation of PVA at the interface of both phenomena may be at the point of the observed shoulder. The shoulder temperature was increased after freezing–thawing as similar to melting temperature which can be explained in the same way. Calculating the heat of fusion in PVA is difficult due to the simultaneous occurrence of melting and degradation processes thus the overlapping peaks should be deconvoluted which was out of the scope of this report.

DSC diagrams for blend hydrogels of the other compositions, i.e., Dex10, 20 and 30% (w/w) showed that upon higher dextran content, the melting peaks broadened and for Dex20 onwards the second peak was multiplied (Fig. 3c and Table 1). The sharp endothermic peak of melting indicated the presence of homogeneous and more defined crystal structures, and therefore the broadening of the endothermic peaks in the blend hydrogels may elucidate an increased crystal size distribution upon inclusion of higher dextran content. This means that formation of the PVA crystals has been affected by the presence of dextran. Multiplying peaks of melting process indicates that there may be two distinct phases which are partially miscible because the second peak of Dex10 showed as

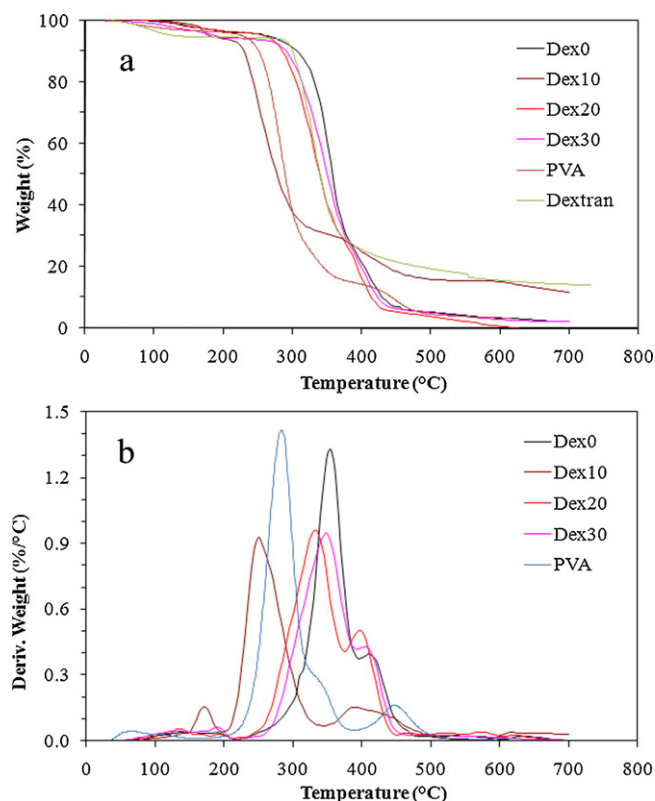


Fig. 4. TGA thermograms of PVA based hydrogels containing various amounts of dextran showing changes in thermal degradation profile as weight percent (a) and differential form showing a three stage degradation process (b).

a single peak, whereas for higher dextran contents the multiple peaks are near each other due to partially immiscible phases of PVA and dextran. First, with introducing dextran in the PVA hydrogel structure melting and shoulder temperatures have shifted to higher temperature both in the higher and lower temperature side peaks as depicted in Fig. 3d. Increase in dextran content above 10% (w/w) did not affect melting and shoulder temperatures. This shows that there is a critical value of 10% (w/w) or less for dextran content to obtain a miscible blend. According to the calculation of surface area of crystalline domains for all samples in their melting range, it seems that the hydrogel blend with 10% (w/w) dextran has crystallinity a little higher than the other hydrogels and this is another reason for partial miscibility of dextran and PVA in Dex10. Melting and degradation points of hydrogels beyond 240 °C were significantly influenced by their dextran contents in the composition as with less dextran content, sharper degradation profile was observed (Fig. 3d) and with higher dextran content the peak became broader and multistage and shifted to higher temperature although; it is difficult to give one argument to explain this behavior. In comparison with TGA results it is obvious that melting may occur simultaneously with degradation.

### 3.2.2. Thermal gravimetric analysis

Thermal degradation of xerogels was evaluated by TGA as illustrated in Fig. 4. A three-stage thermal degradation profile was observed for all samples except dextran which resulted in three corresponding weight loss peaks in thermogravimetric (DTG) derivative curves however, the first stage of degradation in neat PVA and Dex0 specimens was negligible. Each sample showed its own temperature range for each stage according to the composition. The overall temperature range for first stage was up to 200 °C; the second stage from 200 °C to 400 °C and the third stage from 400 °C up to 600 °C. The amount of weight loss and temperature at

maximum weight loss rate for each stage are listed in Table 2 for all the samples. In PVA and its blends, the first weight loss stage (Table 2) varies with no specific trend for different compositions and may be attributed to their residual water content in the network and the remaining acetate functional groups which are more susceptible for cleavage than the OH functional group. The second phase is accompanied with a physical phenomenon such as melting of crystallites followed by degradation of the xerogel blend bulk as elucidated by DSC studies (Fig. 3) where the chemical pyrolytic reactions occur at the same time (Fig. 4). According to TGA results (Fig. 4), PVA thermal stability has improved upon freezing–thawing cycles as degradation temperature of 280 °C is increased to 350 °C and weight loss of 80.01% drops to 74.87% with lower rate of degradation compared to pure PVA. This phenomenon is based on the thermal stability and morphological characteristics such as more ordered crystalline domains of an emerged crystalline polymer upon freezing–thawing cycles compared to an amorphous state of the same polymer. Thus it is logical that pseudo-crosslinking due to the induced crystallinity in PVA itself can improve its thermal stability.

Thermal decomposition of PVA *per se* is a complex process which may end to different products, e.g., water, acetaldehyde, alcohols, acetone and acids in different proportions according to experimental conditions (Patachia, Vasile, & Mavru, 1985). The presence of dextran in the network negatively affects thermal stability of the freeze–thawed PVA xerogels for maximum content of 20% (w/w) of dextran thus; degradation temperatures of the samples are reduced from 350 °C for Dex0 to 250 °C, 330 °C and 345 °C for Dex10, 20 and 30 specimens, respectively. This effect is reversed at higher dextran loading, i.e., 30% (w/w) (Fig. 4 and Table 2). In contrast, the weight loss percentage is lowered in the samples by introduction of dextran (max 10%, w/w or even less) into PVA hydrogels and the weight loss process simultaneously undergoes a slower rate of thermal decomposition compared to Dex0. By further increase in dextran content beyond 10% (w/w) there is a negative effect and the weight loss is intensified. This can be attributed to partial miscibility of dextran and PVA in dextran weight ratio below 10% (w/w) as a consequence of molecular interactions between the two components. As it is evident in Fig. 4b degradation peaks are even sharper in Dex10 compared to Dex20 and Dex30 indicating xerogel blend homogeneity for Dex10 samples. Interpretation of the chemical degradation routes and mechanisms involved for the observed phenomena of these two reverse effects need to be explored further by instrumental techniques capable of characterization of degradation products such as pyrolytic GC–MS, etc., to provide detailed molecular and kinetics of the observed degradations which are beyond the scope of this report.

### 3.3. Fourier-transform infrared spectroscopy

In order to elucidate the formation mechanism for PVA/dextran blend hydrogels, FTIR spectra of the samples were quantitatively studied after extraction of sol fraction. Fig. 5a shows the infrared spectra each of pure PVA and frozen–thawed PVA xerogels. Table 3 provides the wavenumbers for specific signals for PVA, dextran and their freeze–thaw blends. The O–H stretching band in the IR spectrum is by far the most characteristic feature of alcohols and appears at wavenumbers beyond 3000  $\text{cm}^{-1}$ . The signal which has appeared at 3200–3500  $\text{cm}^{-1}$  is attributed to O–H stretching due to the intermolecular and intramolecular hydrogen bonds. This characteristic signal can be seen in all samples except Dex0 because of the presence of OH in both PVA and dextran. In Dex10, this characteristic signal has shifted to higher wavenumbers which is accounted for stronger hydrogen bonding between the two polymers (Table 3). The reason for the absence of any signal in 3200–3500  $\text{cm}^{-1}$  range for Dex0 may be due to the pos-



**Table 2**

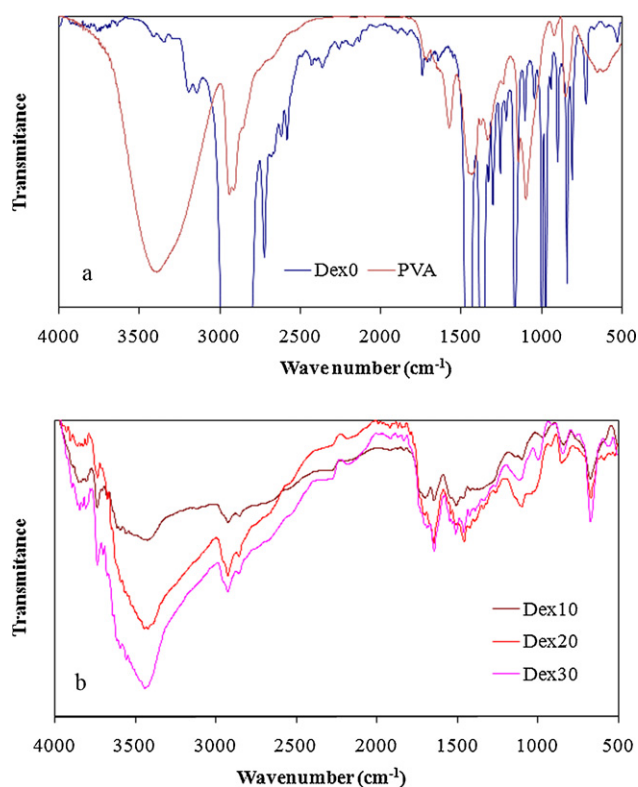
Peak temperatures of thermal degradation and the corresponding weight loss percentage for PVA–dextran xerogels.

Sample	First stage (<200 °C)		Second stage (200–400 °C)		Third stage (400–600 °C)		Remained mass (%)
	Temp. (°C)	Weight loss (%)	Temp. (°C)	Weight loss (%)	Temp. (°C)	Weight loss (%)	
PVA	–	3.82	280	80.01	438	10.51	5.6
Dex0	–	3.66	350	74.87	420	18.18	3.29
Dex10	165	5.78	250	69.22	380	9.85	18.38
Dex20	125	3.35	330	78.29	390	16.36	0
Dex30	180	3.6	345	74.72	395	16.8	2.88
Dextran	–	5.38	340	69.62	540	9.48	15.52

**Table 3**

FT-IR spectral characteristics for PVA–dextran blends.

	3900–1700 (cm <sup>-1</sup> )			1700–1000 (cm <sup>-1</sup> )		
PVA	3436	2944 2917	1733	1579	1455 1344	1145 1103 1040
Dextran	3448	2925	–	1675	1473 1382	1172 1025
Dex0	–	2973 2848 2724	1743	–	1465 1376	1166 998 973
Dex10	3853 3737 3455	2929 2890	1714	1648	1511 1392	1155 1110
Dex20	3739 3455	2931 2896	1714	1652	1476	1126
Dex30	3852 3737 3455	2931 861	1707	1646	1513 1504	1139 1012

**Fig. 5.** FTIR spectra of neat PVA and freeze–thawed PVA (Dex0) samples (a); changes in the spectra of PVA xerogels due to inclusion of 10 (Dex10), 20 (Dex20) and 30 (Dex30) % (w/w) of dextran (b).

sible dehydration of PVA since the appropriate signal intensity has increased with increased dextran content in frozen–thawed PVA blends (Fig. 5b). The vibrational band, observed between 2840 and 3000 cm<sup>-1</sup> in all the compositions, refers to the C–H stretching of alkyl groups (Table 3). The peaks at 1733 and 1579 cm<sup>-1</sup> in PVA spectra are assigned to the C=O stretching from acetate and carboxylic acid functional groups remaining from polyvinyl acetate precursor. The signal intensity is low in all the samples upon high degree of PVA hydrolysis and it is shifted to 1743, 1714, 1714 and 1707 cm<sup>-1</sup> in Dex0, 10, 20 and 30. This can be attributed to the presence of intermolecular hydrogen bonding in PVA and it is most apparent in Dex0 sample where hydrogen bonding is strongest. Absorption peak of C–C bond of dextran appears in 1675 cm<sup>-1</sup> which shows shifts to lower wavenumbers but within a narrow range (Table 3). The peaks appeared at 1455 and 1344 cm<sup>-1</sup> may also be attributed to the C–O–H bonds (*d* (CH–OH) resonance) (Krimm, Liang, & Sutherland, 2003).

In the discussion of PVA gels, Hassan *et al.* have referred to an absorption peak at 1141 cm<sup>-1</sup>, which is indicative of PVA crystallinity and arises from a C–C stretching mode and intensifies with an increased degree of crystallinity (Peppas, 1987), as it is evident at 1145 cm<sup>-1</sup> in PVA and its physically crosslinked blends with dextran (Fig. 5a) which indicates that a crystalline effect has occurred. Signal at 1166 cm<sup>-1</sup> wavenumber with strong intensity is attributed to C–O in stretching mode and it is very sensitive to heat treatment of PVA samples and hence their crystallinity. This band is associated with the  $\nu$ (C–O) mode of a portion of the chain, where due to OH functional groups two hydrogen bonds come into intramolecular interactions on the same plane of carbon chain (Peppas, 1977) and will not be affected by bound water content of xerogels. Weak signals at 1041 cm<sup>-1</sup> which can be attributed to

the amorphous syndiotactic and atactic chain segments are characteristic of higher crystallinity of PVA xerogels. Characteristic C—OH stretching at  $1103\text{ cm}^{-1}$  (weak intensity) is also confirmed (Kim et al., 2003a).

#### 4. Conclusion

The overall morphology and thermal properties of PVA-based blend xerogels prepared by freeze–thaw technique were investigated. The results showed that introduction of dextran in the physically crosslinked PVA network significantly affected its molecular structure and thermal properties of the xerogels. SEM results indicated that morphology was strongly dependent on dextran content. Blend homogeneity was observed for 10% (w/w) dextran loaded xerogels however; increasing in dextran content to maximum 20% (w/w) resulted in xerogels owing to porous structure in contrast to smooth surface and non-porous structure of PVA xerogels without dextran. A channeled morphology is evident for samples of higher dextran content, i.e., 30% (w/w). Virgin PVA xerogels show lower  $T_g$  in comparison to neat PVA upon freezing–thawing cycles although it is increased by 10% (w/w) dextran content and it remains constant by 20 and 30% (w/w) dextran in the blended specimens. This is attributed to the higher  $T_g$  of dextran relative to PVA and their miscibility at approximately 10% (w/w) dextran content. The crystallite size distribution of PVA was broadened by higher dextran content, i.e., the dextran perturbed crystal formation in freeze–thawed PVA and not necessarily decreasing the degree of crystallinity. Physical crosslinking of PVA itself has improved thermal stability of PVA-based materials. Higher thermal stability of xerogels containing dextran can be due to the higher degradation temperature of dextran although the weight loss is at the lowest at 10% (w/w) dextran content, because of its miscibility in PVA. FTIR results indicate that absorptions related to hydrogen bonds in Dex10 samples have shifted to higher wavenumbers. On the whole, the results suggest that there is a threshold for miscibility of dextran in PVA which definitely stands under 10% (w/w) dextran content for conditions used throughout this study.

#### References

- Berger, J., Reist, M., Mayer, J. M., Felt, O., & Gurnyb, R. (2004). Structure and interactions in chitosan hydrogels formed by complexation or aggregation for biomedical applications. *European Journal of Pharmaceutics and Biopharmaceutics*, 57, 35–52.
- Bolton, S. (1991). *Pharmaceutical statistics practical and clinical applications*. New York: Marcel Dekker., p. 650.
- Cascone, M. G., Maltinti, S., & Barbani, N. (1999). Effect of chitosan and dextran on the properties of poly(vinyl alcohol) hydrogels. *Journal of Materials Science Materials in Medicine*, 10, 431–435.
- Dai, S., & Barbani, T. A. (1999). Hydrogel membranes with mesh size asymmetry based on the gradient crosslinking of poly(vinyl alcohol). *Journal of Membrane Science*, 156, 67–79.
- De Jong, S. J., van Eerdenbrugh, B., van Nostrum, C. F., Kettenes-van den Bosch, J. J., & Hennink, W. E. (2001). Physically crosslinked dextran hydrogels by stereocomplex formation of lactic acid oligomers: Degradation and protein release behavior. *Journal of Controlled Release*, 71, 261–275.
- Hassan, C. M., & Peppas, N. A. (2000). Structure and morphology of freeze/thawed PVA hydrogels. *Macromolecules*, 33, 2472–2479.
- Hennink, W. E., De Jong, S. J., Bos, G. W., Veldhuis, T. F. J., & van Nostrum, C. F. (2004). Biodegradable dextran hydrogels crosslinked by stereocomplex formation for the controlled release of pharmaceutical proteins. *International Journal of Pharmaceutics*, 277, 99–104.
- Hennink, W. E., & van Nostrum, C. F. (2002). Novel crosslinking methods to design hydrogels. *Advanced Drug Delivery Reviews*, 54, 13–36.
- Kim, S. J., Park, S. J., & Kim, S. I. (2003a). Swelling behavior of interpenetrating polymer network hydrogels composed of poly(vinyl alcohol) and chitosan. *Reactive and Functional Polymers*, 55, 53–59.
- Kim, S. J., Park, S. J., & Kim, S. I. (2003b). Synthesis and characteristics of interpenetrating polymer network hydrogels composed of poly(vinyl alcohol) and poly(Nisopropylacrylamide). *Reactive and Functional Polymers*, 55, 61–67.
- Korsmeyer, R., & Peppas, N. A. (1981). Effect of the morphology of hydrophilic polymeric matrices on the diffusion and release of water soluble drugs. *Journal of Membrane Science*, 9, 211–227.
- Krimm, S., Liang, C. Y., & Sutherland, G. B. B. M. (2003). Infrared spectra of high polymers. V. Polyvinyl alcohol. *Journal of Polymer Science Polymer Chemistry*, 22, 227–247.
- Lucke, A., Tebmar, J., Schnell, E., Schmeer, G., & Pferich, A. (2000). Surface properties relevant to their use as biomaterials. *Biomaterials*, 21, 2361–2370.
- Manabu, M., & Takehisa, M. (2002). Liquid acrylate-endcapped biodegradable poly(e-caprolactone-co-trimethylene carbonate). I. Preparation and visible light-induced photocuring characteristics. *Journal of Biomedical Materials Research*, 62, 387–394.
- Marten, F. L. (1985). In H. F. Mark, Bikales N.M., G. Overberger, G. Menges, & J. I. Kroschwitz (Eds.), *Encyclopedia of polymer science and engineering*. New York: John Wiley and Sons, 17, p. 167.
- Molina, I., Suming, L., Martinez, M. B., & Vert, M. (2001). Protein release from physically crosslinked hydrogels of the PLA/PEO/PLA triblock copolymer-type. *Biomaterials*, 22, 363–369.
- Park, K. R., & ChangNho, Y. (2003). Synthesis of PVA/PVP hydrogels having two-layer by radiation and their physical properties. *Radiation Physics and Chemistry*, 67, 361–365.
- Patachia, S., Vasile, C., & Mavru, E. (1985). Study of the compatibility in the poly(vinyl-chloride)–poly(vinyl-alcohol) system. *Polymer Bulletin*, 13, 301–306.
- Peppas, N. A. (1975). Turbidimetric studies of aqueous poly(vinyl alcohol) solutions. *Macromolecular Chemistry*, 176, 3433–3440.
- Peppas, N. A. (1977). Infrared spectroscopy of semicrystalline poly(vinyl alcohol) networks. *Macromolecular Chemistry*, 178, 595–601.
- Peppas, N. A. (1987). *Hydrogels in medicine in pharmacy*. Boca Raton, FL: CRC Press., pp. 1–48.
- Peppas, N. A., & Benner, R. E. (1980). Proposed method of intracordal injection and gelation of poly(vinyl alcohol) solution in vocal cords: Polymer considerations. *Biomaterials*, 1, 158–162.
- Peppas, N. A., & Scott, J. E. (1992). Controlled release from poly(vinyl alcohol) gels prepared by freeze–thawing processes. *Journal of Controlled Release*, 8, 95–100.
- Soppimath, K. S., & Aminabhavi, T. M. (2002). Water transport and drug release study from cross-linked polyacrylamide grafted guar gum hydrogel microspheres for the controlled release application. *European Journal of Pharmaceutics and Biopharmaceutics*, 53, 87–98.
- Teramoto, N., Saitoh, M., Kuroiwa, J., Shibata, M., & Yosomiya, R. (2001). Morphology and mechanical properties of pullulan/poly(vinyl alcohol) blends crosslinked with glyoxal. *Journal of Applied Polymer Science*, 82, 2273–2280.
- Van Tomme, S. R., van Steenberghe, M. J., De Smedt, S. C., van Nostrum, C. F., & Wim, E. (2005). Self-gelling hydrogels based on oppositely charged dextran microsphere. *Biomaterials*, 26, 2129–2135.
- Wichterle, O., & Lim, D. (1960). Hydrophilic gels for biological use. *Nature*, 185, 117–118.
- Yokoyama, F., Masada, I., Shimamura, K., Ikawa, T., & Monobe, K. (1985). Morphology and structure of highly elastic poly(vinyl alcohol) hydrogel prepared by repeated freezing–and melting. *Colloid Polym. Sci.*, 264, 595–601.
- Yoshii, F., Zhanshan, Y., Isobe, K., Shinozaki, K., & Makuuchi, K. (1999). Electron beam crosslinked PEO and PEO/PVA hydrogels for wound dressing. *Radiation Physics and Chemistry*, 55, 133–138.
- Zhao, L., Mitomo, H., Zhai, M., Yoshii, F., Nagasawa, N., & Kume, T. (2003). Synthesis of antibacterial PVA/CM-chitosan blend hydrogels with electron beam irradiation. *Carbohydrate Polymers*, 53, 439–446.